Volume 19
Number 6
June 1980

Inorganic Chemistry

Contribution from the Department of Chemistry,
Colorado State University, Fort Collins, Colorado 80523

Crystal and Molecular Structure of a Nitroxyl Radical Complex of Copper(II): Bis(hexafluoroacetylacetonato)(4-hydroxy-2,2,6,6-tetramethylpiperidinyl-*N*-oxy)copper(II)

OREN P. ANDERSON*[1] and THOMAS C. KUECHLER

Received September 14, 1979

The crystal and molecular structure of the adduct between bis(hexafluoroacetylacetonato)copper(II) (Cu(hfac)$_2$) and the nitroxyl radical 4-hydroxy-2,2,6,6-tetramethylpiperidinyl-*N*-oxy (TMPO–OH) has been determined from three-dimensional single-crystal X-ray diffraction data, collected by counter techniques. The green/brown dichroic crystals of Cu(hfac)$_2$-(TMPO–OH) are monoclinic, space group $P2_1/n$, with four formula units in the unit cell (a = 10.482 (3) Å, b = 15.565 (5) Å, c = 16.702 (5) Å, β = 97.75 (2)°). The structure has been refined by least-squares methods to $R = 0.061$ (R_w = 0.072) for 2656 unique reflections with $F^2 > 3\sigma(F^2)$. Binding of the nitroxyl radical to the approximately square-planar Cu(hfac)$_2$ species through both the nitroxyl group and the 4-hydroxy moiety results in formation of polymeric chains comprised of Cu(hfac)$_2$ units connected by TMPO–OH radicals in the crystal lattice. The coordination geometry about each copper(II) ion corresponds to a tetragonally distorted octahedron, with four short bonds from copper(II) to the hexafluoroacetylacetonate oxygen atoms (Cu–O(av) = 1.947 (4) Å) and much longer bonds to the nitroxyl oxygen (Cu–O1 = 2.439 (6) Å) and hydroxyl oxygen (Cu–O6 = 2.414 (4) Å) atoms of the nitroxyl radical ligand. The observed conformation of the nitroxyl radical ligand, together with thermal parameters of the atoms of this species, suggests the presence of more than one conformation for the nitroxyl radical in the solid state.

Introduction

Nitroxyl radicals are stable free radicals which can function as Lewis bases. These properties have led to the use of nitroxyl radicals as spin probes in biochemical systems[2,3] and as ligands for a variety of transition metals.[3-7] In transition-metal systems nitroxyl radical ligands possess the potential of acting as a probe of the metal–ligand bonding, as was recently demonstrated by an electron spin resonance study of the adduct between the 2,2,6,6-tetramethylpiperidinyl-*N*-oxy radical and the rhodium(II) trifluoroacetate dimer.[5] In addition, binding of the nitroxyl radical ligand to a paramagnetic transition-metal ion would be expected to lead to significant magnetic interactions between the unpaired electrons on the radical ligand and on the metal. Several cases have been studied[4] in order to explore these magnetic-exchange interactions in such complexes. In all of these previously studied cases, the magnitudes of the magnetic interactions between the nitroxyl radical ligands and the paramagnetic metal ions have been found to be large. Recent detailed studies of the Cu(hfac)$_2$·TMPO and VO(hfac)$_2$·TMPO (hfac = hexafluoroacetylacetonate, TMPO = 2,2,6,6-tetramethylpiperidinyl-*N*-oxy radical) adducts verified the existence of a large magnetic-exchange interaction between the unpaired electrons on the metal atoms and the radical ligand and also showed that the resultant spin pairing did not contribute to the stability of these adducts.[6,7]

It has become common practice in the study of exchange interactions to relate the magnetic susceptibility results to the molecular structure as determined by X-ray crystallography.[8] In this manner, the exchange pathways responsible for the observed interaction may often be deduced. However, no crystal structures have been reported for the case in which a nitroxyl radical is directly coordinated to a paramagnetic metal ion, even though attempts to determine such structures have been made.[9] This paper reports the crystal and molecular structure of the adduct between bis(hexafluoroacetylacetonato)copper(II) and the 4-hydroxy-2,2,6,6-tetramethylpiperidinyl-*N*-oxy radical (TMPO–OH). The room-temperature magnetic susceptibility observed for this com-

---

(1) To whom correspondence should be addressed.

(2) (a) Griffith, O. H.; Waggoner, A. S. *Acc. Chem. Res.* **1969**, *2*, 17. (b) Likhtenshtein, G. I. "Spin Labeling Methods in Molecular Biology"; Wiley: New York, 1969. (c) Berliner, L. J. "Spin Labeling: Theory and Applications"; Academic Press: New York, 1976. (d) Dugas, H. *Acc. Chem. Res.* **1977**, *10*, 47.

(3) Eaton, S. S.; Eaton, G. R. *Coord. Chem. Rev.* **1978**, *26*, 207.

(4) (a) Brown, D. G.; Maier, T.; Drago, R. S. *Inorg. Chem.* **1971**, *10*, 2804. (b) Zelonka, R. A.; Baird, M. C. *J. Am. Chem. Soc.* **1971**, *93*, 6066. (c) Karayannis, N. M.; Paleos, C. M.; Mikulski, C. M; Pytlewski, L. L.; Blum, H.; Labes, M. M. *Inorg. Chim. Acta* **1973**, *7*, 74. (d) Jahr, D.; Rebhan, K. H.; Schwarzhans, K. E.; Wiedemann, J. *Z. Naturforsch., B* **1973**, *28*, 55. (e) Richardson, P. F.; Kreilick, R. W. *J. Am. Chem. Soc.* **1977**, *99*, 8183. (f) Richardson, P. F.; Kreilick, R. W. *Chem. Phys. Lett.* **1977**, *50*, 333.

(5) Richman, R. M.; Kuechler, T. C.; Tanner, S. P.; Drago, R. S. *J. Am. Chem. Soc.* **1977**, *99*, 1055.

(6) Lim, Y. Y.; Drago, R. S. *Inorg. Chem.* **1972**, *11*, 1334.

(7) Drago, R. S.; Kuechler, T. C.; Kroeger, M. K., submitted for publication in *Inorg. Chem.*

(8) (a) Felthouse, T. R.; Hendrickson, D. N. *Inorg. Chem.* **1978**, *17*, 2636. (b) Pierpont, C. G.; Francesconi, L. C.; Hendrickson, D. N. *Ibid.* **1977**, *16*, 2367. (c) Hay, P. J.; Thibeault, J. C; Hoffmann, R. *J. Am. Chem. Soc.* **1975**, *97*, 4884.

(9) The present authors have attempted to determine the crystal and molecular structure of the vanadyl complex [VO(hfac)$_2$(TMPO)]. Preliminary precession and Weissenberg photographs revealed a lattice structure modulation which prevented assignment of a space group and solution of the structure. Other workers have also reported unsuccessful attempts to determine the structures of nitroxyl radical complexes (see ref 4a and 6).

0020-1669/80/1319-1417$01.00/0 © 1980 American Chemical Society

pound suggests that the magnetic-exchange interaction between the nitroxyl radical and the paramagnetic transition-metal ion is very small.

Experimental Section

Preparation of Cu(hfac)$_2$·TMPO–OH. Cu(hfac)$_2$·2H$_2$O and TMPO–OH were prepared by previously reported procedures.[10,11] Cu(hfac)$_2$·2H$_2$O was purified by sublimation. The adduct was prepared by adding a solution of 0.17 g (1 mmol) of TMPO–OH in methylene chloride to a solution of 0.51 g (1 mmol) of Cu(hfac)$_2$·2H$_2$O in methylene chloride. The resulting solution was then cooled for 12 h in a freezer, during which time the adduct crystallized as large, blocky crystals. The crystals were dichroic, appearing dark green or brown when viewed through different faces. Anal. Calcd for Cu(C$_5$HO$_2$F$_6$)$_2$(C$_9$H$_{18}$NO$_2$): C, 35.11; H, 3.10; N, 2.16; Cu, 9.78; F, 35.08. Found: C, 35.22; H, 3.14; N, 2.18; Cu, 9.93; F, 35.05. The magnetic susceptibility was determined at 21 °C by using a Cahn 7600 Faraday system with Hg[Co(NCS)$_4$] as calibrant.

Crystal Data. For Cu(C$_5$HO$_2$F$_6$)$_2$(C$_9$H$_{18}$NO$_2$) (mol wt 649.90, monoclinic) $a = 10.482$ (3) Å, $b = 15.565(5)$ Å, $c = 16.702$ (5) Å, $\beta = 97.75$ (2)°, $V = 2700.1$ Å^3, $\rho_{\text{obsd}} = 1.60$ g cm^{-3}, $\rho_{\text{calcd}} = 1.60$ g cm^{-3}, $Z = 4$, and $F(000) = 1304$ (space group $P2_1/n$, Mo Kα radiation, λ_1 0.709 30 Å, λ_2 0.713 59 Å, μ(Mo Kα) = 9.23 cm^{-1}).

Data Collection and Reduction. Preliminary Weissenberg and precession photographs revealed Laue symmetry $2/m$ and exhibited systematic absences ($h0l$, $h + l = 2n + 1$; $0k0$, $k = 2n + 1$) which were only consistent with the monoclinic space group $P2_1/n$ (a variant of $P2_1/c$, No. 14).[12] The crystal chosen for data collection was mounted on the Enraf-Nonius CAD-3 diffractometer with the b axis nearly coincident with the diffractometer ϕ axis. The orientation matrix for data collection and the unit cell parameters reported above were obtained from least-squares calculations[13] on the automatically determined[14] 2θ, χ, and ϕ settings (at 20 (1) °C) of 32 reflections with 2θ values in the range 18–25°. The measured density reported was obtained by neutral buoyancy in a mixture of carbon tetrachloride and 1,2-dibromoethane.

The intensities of 4914 reflections with $4.5° < \theta < 25°$ were measured by θ–2θ scans, employing Zr-filtered Mo Kα radiation. The total scan range was 1.00° (in θ) at a constant scan rate of 10° min^{-1}. The number of scans for a given reflection varied according to the intensity, with weak reflections being scanned a maximum of five times. Background was counted at both ends of the scan, for a total time equal to the scan time. The takeoff angle was 3.5°, and zirconium foil attenuators were inserted automatically if the peak count rate exceeded 2500 counts s^{-1}. The intensity of one of three reference reflections (0, 0, 10; 080; 600) was measured every 25 reflections. None of these reference reflections showed any significant changes in intensity during the course of data collection.

Lorentz and polarization corrections were applied to the observed data. The uncertainty parameter g in the formula[15] for the standard deviation in the intensity was taken as 0.04. After averaging of equivalent reflections, the 2656 reflections for which $F_o^2 > 3\sigma(F_o^2)$ were employed in the solution and refinement of the structure. No absorption correction was applied to the data, due to the low absorption coefficient reported above. The crystal used for data collection had dimensions of 0.20 mm ($\{10\bar{1}\}\rightarrow\{\bar{1}01\}$) × 0.25 mm ($\{0\bar{1}\bar{1}\}\rightarrow\{011\}$) × 0.30 mm ($\{01\bar{1}\}\rightarrow\{0\bar{1}1\}$).

Structure Solution and Refinement. The position of the copper(II) ion was assigned from the double-intensity nonorigin peaks appearing in the Harker sections of the Patterson map. The positions of all nonhydrogen atoms were then obtained from a series of Fourier syntheses phased by the atoms in known positions. Scattering factors for copper(II), carbon, nitrogen, oxygen, and fluorine were taken from ref 16.

Two of the CF$_3$ groups were found to be disordered about the C–C bond (C13–C14 and C18–C19) connecting them to the acetylacetonate ligand. The nature of the disorder was such that two separate sets of fluorine atoms could be seen in a difference Fourier map in each case. On the basis of the interpolated heights of the peaks for these partial atoms in the Fourier map, fixed population parameters of 0.55 and 0.45 were assigned to the atoms F4–F6 and F4′–F6′, respectively. Corresponding parameters were 0.70 and 0.30 for atoms F10–F12 and F10′–F12′, respectively.

Due to the large number of atoms in the asymmetric unit and to computer limitations of the refinement was calculated in two parts. In part A of each cycle, the positional and thermal parameters of the atoms of the nitroxyl radical, Cu(II), and the oxygen atoms of the hexafluoroacetylacetonate ligand were varied. In part B of each cycle, the positional and thermal parameters of Cu(II) and all of the atoms of the hexafluoroacetylacetonate ligands were allowed to vary. Three cycles of least-squares refinement (on F, each cycle comprised of a part A/part B pair of calculations) with idealized CF$_3$ rigid groups and anisotropic thermal parameters for all nongroup atoms lowered R $(=\sum||F_o| - |F_c||/\sum|F_o|)$ from its initial value of 0.239 to 0.119 and R_w $(=[\sum w(|F_o| - |F_c|)^2/\sum wF_o^2]^{1/2})$ from 0.306 to 0.145. The NUCLS refinement program minimizes $\sum w(|F_o| - |F_c|)^2$, where F_o and F_c are the observed and calculated structure amplitudes, respectively, and w is the weight $(=4F_o^2/\sigma^2(F_o^2))$.

Examination of a difference Fourier map calculated at this point revealed peaks in the immediate vicinity of each fluorine atom. The profiles of these peaks suggested that a principal reason for the relatively high R factors at this point was inadequate representation of the anisotropic thermal motion of the fluorine atoms by the isotropic rigid group model. It was, therefore, deemed necessary to replace these rigid CF$_3$ groups with fluorine atoms for which the positional and anisotropic thermal parameters were individually variable. To compensate for the lower data/parameter ratio which resulted from this conversion, we converted the thermal parameters of the carbon and oxygen atoms of the hexafluoroacetylacetonate ligands back to isotropic parameters for all subsequent refinement cycles. This was felt to be justified by the essentially isotropic character of the anisotropic thermal parameters for these atoms at this stage of the refinement calculations. The final refinement cycles were based on a total of 336 adjustable parameters, giving a final data/parameter ratio of 7.9. Three cycles of least-squares refinement (each cycle calculated in two parts as before) then reduced R to its final value of 0.061 and R_w to 0.072.

On the final cycle of refinement, no parameter shift for any nonfluorine atom was greater than 55% of the standard deviaiton in that parameter (and most were much less). For the CF$_3$ groups which showed no disorder (F1, F2, F3; F7, F8, F9), no shift was larger than 75% of the corresponding standard deviation. For the CF$_3$ groups modeled with partial occupancy (total of 12 partial fluorines) five positional parameters had shifts greater than one standard deviation. The largest shift was in the y parameter of F12 and was equal to 1.4σ. All of these calculated shifts had decreased by a factor of approximately 4 as compared with results from the previous cycle, so that another cycle of refinement was not deemed necessary. A final difference Fourier map showed no peak higher than 0.40 e Å^{-3} and no depression lower than 0.35 e Å^{-3}. The most pronounced peaks in this map were either associated with the CF$_3$ groups or appeared at positions where hydrogen atoms might have been expected.

Final atomic positional parameters and isotropic thermal parameters are listed in Table I. Table II lists the final anisotropic thermal parameters, while Table VI (included as supplementary information in the microfilm edition of this journal) contains a listing of the F_o and final F_c values for the title compound.

Results and Discussion

Table III lists the calculated bond lengths and angles involving copper(II), while the bond lengths and angles char-

---

(10) Belford, R. L.; Martell, A. E.; Calvin, M. *J. Inorg. Nucl. Chem.* **1956**, *2*, 11.

(11) Briere, R.; Lemaire, H.; Rassat, A. *Bull. Soc. Chim. Fr.* **1965**, 3273.

(12) "International Tables for X-Ray Crystallography"; Kynoch Press: Birmingham, England, 1969; Vol. I.

(13) The following programs were used in this structure determination: Zalkin's FORDAP Fourier program; Ibers' NUCLS, a group/nongroup least-squares version of the Busing–Levy ORFLS program; Ibers' CELREF for least-squares refinement of cell parameters; ORFFE, Busing and Levy's function and error program; ORTEP, Johnson's thermal ellipsoid plot program. The program for data reduction and Lp correction was locally written for the CDC Cyber 171/172 computers at Colorado State University.

(14) Optimum angular settings were determined by using the automated routines incorporated in the Enraf-Nonius diffractometer package.

(15) (a) Corfield, P. W. R.; Doedens, R. J.; Ibers, J. A. *Inorg. Chem.* **1967**, *6*, 197. (b) Anderson, O. P.; Packard, A. B.; Wicholas, M. *Ibid.* **1976**, *15*, 1613.

(16) "International Tables for X-Ray Crystallography"; Kynoch Press: Birmingham England, 1974; Vol. IV.

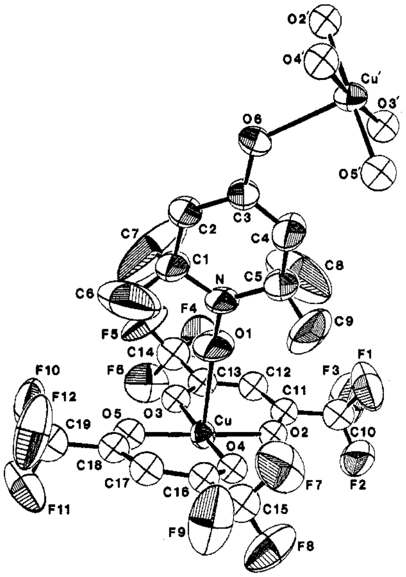

Figure 1. A view of the $Cu(hfac)_2(TMPO–OH)$ complex, showing the interaction of the TMPO–OH radical with two copper(II) ions. Partial fluorine atoms corresponding to the minor orientations of the CF_3 groups have been omitted for clarity. Atoms which are not shaded were refined with isotropic thermal parameters.

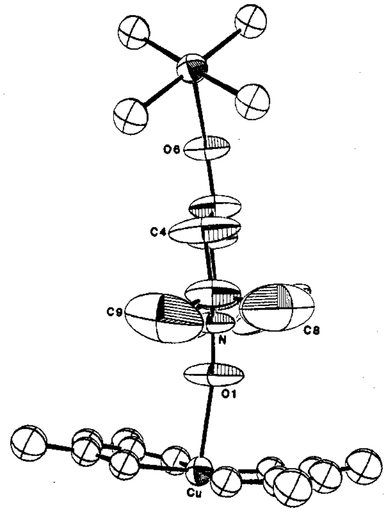

Figure 2. A view of the same unit as in Figure 1, showing the large amplitude thermal motion of the atoms of the TMPO–OH radical ligand.

acteristic of the hexafluoroacetylacetonate and nitroxyl radical ligands are reported in Table IV. The estimated standard deviations reported in these tables include the appropriate contributions from the standard deviations in the unit cell parameters.

Figures 1 and 2 show all the bonding interactions important for Cu(II) in this compound. Six atoms are bound to each copper(II) ion at the corners of a tetragonally distorted octahedron. Four of these atoms are the oxygen atoms of the two hexafluoroacetylacetonate ligands, which occupy the coplanar (see Table V) equatorial coordination sites at bonding distances which are equal within experimental error (average Cu–O(hfac) = 1.947 (2) Å. The axial coordination sites are occupied by oxygen atoms of the TMPO–OH radical ligand.

Actually, as can clearly be seen in Figures 1, 2, and 3, each $Cu(hfac)_2$ unit is bonded to two TMPO–OH radical ligands. Thus, one of the axial positions about each copper(II) ion is occupied by the nitroxyl oxygen atom (Cu–O1 = (6) Å) of one TMPO–OH molecule, while the other axial position is occupied by the hydroxyl oxygen atom (Cu–O6 = 2.414 (4) Å) of a second radical ligand. Because of these interactions involving both of the oxygen atoms of each TMPO–OH unit, the crystal structure consists of infinite zigzag chains containing alternating $Cu(hfac)_2$ and TMPO–OH units, with the units of each chain being repeated by the *n*-glide symmetry operation of the $P2_1/n$ space group (see Figure 3). The distance between two copper atoms bridged by a nitroxyl radical in this way is 9.54 Å.

Close inspection of the coordination geometry reveals some small, but significant, deviations from the idealized bonding pattern. The copper(II) ion is displaced 0.05 Å out of the plane defined by the four hexafluoroacetylacetonate oxygen atoms. This displacement is in the direction of the hydroxyl oxygen atom (O6) of the nitroxyl radical. At the same time, the two hexafluoroacetylacetonate rings are bent away from the axial site occupied by the hydroxyl group and toward the axial site occupied by the nitroxyl oxygen atom. This distortion is small, however, since the dihedral angle between these two planes is only 15°. The nitroxyl oxygen atom O1 is not directly over the copper(II) atom, but is displaced slightly toward O3 and O5, with resultant distortions of the O1–Cu–O(hfac) angles (see Table III) from the expected 90° values.

Table I. Atomic Coordinates (Fractional) and Isotropic Thermal Parameters[a]

atom	*x*	*y*	*z*	*U*, Å^2
Cu(II)	0.0043 (1)	−0.1736 (1)	−0.0504 (1)	
N	0.3425 (6)	−0.2135 (4)	0.2687 (3)	
O1	0.4101 (7)	−0.2484 (4)	0.3294 (3)	
O2	0.0527 (4)	−0.0782 (3)	−0.1156 (2)	0.055 (1)
O3	0.1566 (4)	−0.2396 (3)	−0.0652 (2)	0.058 (1)
O4	−0.1553 (4)	−0.1125 (3)	−0.0424 (2)	0.056 (1)
O5	−0.0454 (4)	−0.2700 (3)	0.0133 (3)	0.062 (1)
O6	0.1134 (5)	−0.1038 (3)	0.0686 (3)	
C1	0.3205 (9)	−0.1200 (5)	0.2731 (5)	
C2	0.2317 (9)	−0.0849 (5)	0.2018 (5)	
C3	0.2027 (8)	−0.1378 (5)	0.1325 (5)	
C4	0.2118 (11)	−0.2272 (5)	0.1341 (6)	
C5	0.3039 (10)	−0.2702 (5)	0.1980 (5)	
C6	0.2626 (19)	−0.1006 (10)	0.3511 (7)	
C7	0.4513 (14)	−0.0784 (8)	0.2716 (14)	
C8	0.4392 (17)	−0.2889 (14)	0.1656 (8)	
C9	0.2408 (17)	−0.3466 (7)	0.2282 (9)	
C10	0.1570 (8)	−0.0001 (6)	−0.2040 (5)	0.074 (2)
C11	0.1469 (6)	−0.0791 (4)	−0.1541 (4)	0.055 (2)
C12	0.2380 (7)	−0.1433 (5)	−0.1562 (4)	0.066 (2)
C13	0.2333 (7)	−0.2188 (5)	−0.1107 (4)	0.061 (2)
C14	0.3392 (10)	−0.2880 (7)	−0.1177 (7)	0.088 (3)
C15	−0.3676 (9)	−0.0859 (6)	−0.0203 (6)	0.079 (2)
C16	−0.2469 (6)	−0.1445 (4)	−0.0115 (4)	0.054 (2)
C17	−0.2547 (7)	−0.2218 (5)	0.0264 (4)	0.066 (2)
C18	−0.1518 (6)	−0.2778 (4)	0.0368 (4)	0.056 (2)
C19	−0.1648 (11)	−0.3618 (7)	0.0854 (7)	0.087 (3)
F1	0.0712 (6)	0.0012 (4)	−0.2678 (3)	
F2	0.1406 (6)	0.0703 (3)	−0.1657 (3)	
F3	0.2665 (7)	0.0067 (4)	−0.2334 (4)	
F4	0.4174 (36)	−0.2681 (24)	−0.1670 (23)	
F5	0.2911 (20)	−0.3618 (14)	−0.1296 (34)	
F6	0.4133 (28)	−0.2925 (23)	−0.0487 (15)	
F4′	0.3265 (78)	−0.3171 (51)	−0.1879 (31)	
F5′	0.3387 (96)	−0.3441 (51)	−0.0711 (55)	
F6′	0.4507 (25)	−0.2556 (34)	−0.1112 (95)	
F7	−0.4156 (5)	−0.0767 (4)	−0.0940 (3)	
F8	−0.3342 (5)	−0.0082 (3)	0.0069 (4)	
F9	−0.4592 (5)	−0.1131 (4)	0.0171 (4)	
F10	−0.1022 (39)	−0.4232 (9)	0.0610 (17)	
F11	−0.1197 (34)	−0.3488 (15)	0.1604 (9)	
F12	−0.2819 (15)	−0.3891 (16)	0.0777 (25)	
F10′	−0.0642 (33)	−0.3799 (53)	0.1298 (79)	
F11′	−0.2424 (114)	−0.3518 (28)	0.1369 (52)	
F12′	−0.2011 (103)	−0.4225 (31)	0.0388 (27)	

[a] Standard deviations are in parentheses. The isotropic temperature factor is of the form $\exp[-8\pi^2 U((\sin^2 \theta)/\lambda^2)]$.

Table II. Anisotropic Thermal Parameters ($\times 10^3$, Å^2)[a]

atom	U_{11}	U_{22}	U_{33}	U_{12}	U_{13}	U_{23}
Cu(II)	47 (1)	50 (1)	48 (1)	7 (1)	3 (1)	7 (1)
N	96 (5)	61 (4)	60 (4)	0 (4)	−38 (3)	16 (3)
O1	172 (6)	86 (4)	90 (4)	7 (4)	−69 (4)	26 (3)
O6	96 (4)	62 (3)	56 (3)	12 (3)	−32 (3)	2 (3)
C1	118 (7)	59 (5)	71 (6)	9 (5)	−35 (5)	8 (4)
C2	138 (7)	64 (5)	68 (5)	11 (5)	−57 (5)	1 (7)
C3	124 (7)	58 (5)	64 (5)	31 (5)	−37 (5)	−2 (4)
C4	200 (10)	58 (6)	112 (8)	32 (6)	−96 (7)	−6 (5)
C5	139 (8)	62 (6)	74 (6)	29 (5)	−34 (5)	5 (5)
C6	347 (21)	231 (16)	98 (9)	175 (16)	54 (11)	58 (10)
C7	161 (12)	89 (9)	515 (29)	−50 (9)	−204 (16)	60 (13)
C8	267 (18)	360 (25)	113 (10)	202 (18)	27 (11)	−3 (13)
C9	323 (19)	75 (8)	189 (13)	−90 (10)	−89 (13)	28 (8)
F1	164 (5)	139 (5)	104 (4)	−43 (4)	−29 (4)	58 (4)
F2	200 (6)	67 (3)	116 (4)	−13 (4)	55 (4)	8 (3)
F3	154 (5)	131 (5)	221 (7)	6 (4)	105 (5)	70 (5)
F4	131 (20)	130 (17)	143 (16)	48 (13)	78 (15)	25 (17)
F5	114 (10)	59 (9)	206 (27)	10 (7)	26 (18)	−53 (15)
F6	69 (14)	150 (20)	142 (14)	45 (11)	−13 (11)	−13 (14)
F4′	299 (49)	179 (33)	154 (26)	128 (29)	−14 (24)	−110 (28)
F5′	279 (68)	232 (52)	273 (61)	183 (40)	179 (45)	135 (39)
F6′	39 (10)	224 (39)	743 (116)	5 (13)	52 (30)	−226 (69)
F7	97 (4)	175 (6)	113 (4)	57 (4)	−14 (3)	13 (4)
F8	103 (4)	83 (4)	202 (6)	34 (3)	4 (4)	−28 (4)
F9	95 (4)	135 (5)	251 (7)	49 (4)	101 (5)	76 (5)
F10	169 (21)	68 (8)	155 (18)	37 (13)	63 (15)	45 (9)
F11	175 (20)	188 (17)	72 (6)	−16 (16)	26 (11)	44 (8)
F12	86 (8)	105 (13)	294 (26)	−18 (8)	18 (12)	94 (14)
F10′	62 (16)	194 (61)	265 (101)	−3 (25)	−18 (39)	180 (66)
F11′	304 (68)	102 (25)	234 (43)	80 (37)	236 (51)	106 (28)
F12′	163 (49)	116 (28)	200 (34)	−39 (36)	−26 (41)	24 (21)

[a] In the form $\exp[-2\pi^2(h^2a^{*2}U_{11} + \ldots + 2hka^*b^*U_{12} + \ldots)]$, with standard deviations in parentheses.

Table III. Bond Lengths (Å) and Angles (Deg) Involving Cu(II)[a]

(a) Bond Lengths			
Cu-O1	2.439 (6)	Cu-O4	1.945 (4)
Cu-O2	1.949 (4)	Cu-O5	1.949 (5)
Cu-O3	1.943 (4)	Cu-O6	2.414 (4)
(b) Bond Angles			
O1-Cu-O2	91.5 (2)	O3-Cu-O4	175.6 (2)
O1-Cu-O3	83.1 (2)	O3-Cu-O5	87.0 (2)
O1-Cu-O4	92.5 (2)	O3-Cu-O6	92.1 (2)
O1-Cu-O5	87.6 (2)	O4-Cu-O5	92.5 (2)
O1-Cu-O6	175.2 (2)	O4-Cu-O6	92.3 (2)
O2-Cu-O3	93.0 (2)	O5-Cu-O6	91.6 (2)
O2-Cu-O4	87.5 (2)		
O2-Cu-O5	179.1 (2)		
O2-Cu-O6	89.3 (2)		

[a] Standard deviations are in parentheses.

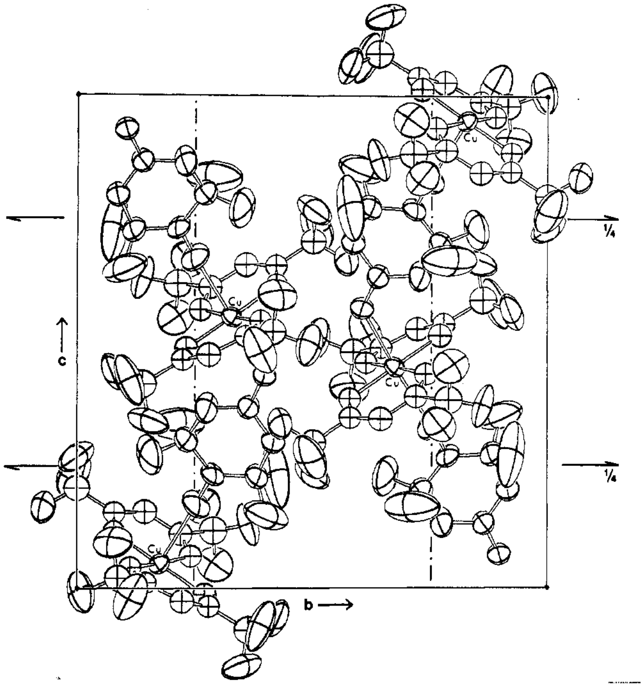

Figure 3. A view (in projection) of the unit cell contents for Cu(hfac)$_2$(TMPO–OH). Minor partial fluorine atoms have been omitted for clarity.

The bond lengths and angles in the hexafluoroacetylacetonate ligand rings fall within the ranges previously observed by Belford, Fenton, and Truter[17] for the closely related structures [Cu(hfac)$_2$·ted]$_\infty$, [Cu(hfac)$_2$·pyr]$_\infty$, and [Cu(hfac)$_2$]$_2$·pyr (where ted = 1,4-diazabicyclo[2.2.2]octane and pyr = pyrazine). As discussed above, the CF$_3$ groups show evidence of disorder and highly anisotropic thermal motion. The average C–F bond length seen in this study is 1.27 (4) Å, the average F–C–F angle is 107 (3)°, and the average C–C–F angle is 112 (2)°. This average C–F bond length is somewhat shorter than would normally be expected,[17,18] although an average C–F distance of 1.29 (2) Å was reported for [Cu(hfac)$_2$]$_2$·pyr.[17] The C–F bond lengths reported in the present study are undoubtedly influenced by the high degree of thermal motion exhibited by the fluorine atoms. As has previously been observed,[17] the CF$_3$ groups show a preferred orientation in which one fluorine atom of the CF$_3$ group lies in the plane of the chelate ring at a maximum distance from the nearest coordinating oxygen atom. In the present structure, the two ordered CF$_3$ groups and one of the orientations of one of the disordered groups exhibit this preferred orientation, as F3, F4, and F9 lie only 0.25, 0.07, and 0.09 Å, respectively,

---

(17) (a) Belford, R. C. E.; Fenton, D. E.; Truter, M. R. *J. Chem. Soc., Dalton Trans.* **1974**, 17; (b) *Ibid.* **1972**, 2208.

(18) "International Tables for X-Ray Crystallography"; Kynoch Press: Birmingham, England, 1968; Vol. III, p 275.

Table IV. Bond Lengths (Å) and Angles (Deg) for Ligands[a]

(a) Bond Lengths for hfac Ligands

O2-C11	1.248 (8)	O4-C16	1.253 (8)
C10-C11	1.499 (11)	C15-C16	1.551 (11)
C11-C12	1.386 (10)	C16-C17	1.368 (10)
C12-C13	1.405 (10)	C17-C18	1.380 (10)
C13-C14	1.562 (13)	C18-C19	1.554 (13)
O3-C13	1.221 (9)	O5-C18	1.237 (8)

(b) Bond Angles for hfac Ligands

Cu-O2-C11	124.2 (4)	Cu-O4-C16	123.2 (4)
O2-C11-C10	113.4 (6)	O4-C16-C15	112.8 (6)
C10-C11-C12	118.5 (7)	C15-C16-C17	117.5 (7)
O2-C11-C12	128.1 (6)	O4-C16-C17	129.6 (6)
C11-C12-C13	120.9 (7)	C16-C17-C18	121.3 (7)
C12-C13-C14	117.3 (7)	C17-C18-C19	118.3 (7)
O3-C13-C12	129.3 (7)	O5-C18-C17	128.3 (7)
O3-C13-C14	113.4 (7)	O5-C18-C19	113.3 (7)
Cu-O3-C13	124.0 (4)	Cu-O5-C18	124.6 (4)

(c) Bond Lengths for Nitroxyl

O1-N	1.276 (8)	C3-O6	1.424 (9)
N-C1	1.477 (10)	C3-C4	1.395 (11)
C1-C6	1.539 (18)	C4-C5	1.498 (13)
C1-C7	1.519 (18)	C5-C8	1.612 (20)
C1-C2	1.512 (11)	C5-C9	1.483 (16)
C2-C3	1.420 (11)	C5-N	1.486 (10)

(d) Bond Angles for Nitroxyl

Cu-O1-N	170.1 (5)	Cu-O6-C3	129.8 (4)
C1-N-C5	126.7 (6)	O6-C3-C2	116.2 (7)
O1-N-C1	117.0 (6)	C2-C3-C4	123.8 (7)
O1-N-C5	116.2 (6)	O6-C3-C4	114.9 (7)
N-C1-C6	108.5 (8)	C3-C4-C5	119.6 (8)
N-C1-C7	105.8 (8)	C4-C5-C8	110.7 (9)
N-C1-C2	113.6 (6)	C4-C5-C9	109.0 (9)
C6-C1-C7	113.0 (12)	N-C5-C4	112.5 (7)
C2-C1-C6	108.9 (9)	C8-C5-C9	115.0 (11)
C2-C1-C7	107.1 (10)	N-C5-C8	102.6 (8)
C1-C2-C3	118.3 (7)	N-C5-C9	107.0 (8)

(e) Bond Lengths Involving Fluorine Atoms

C10-F1	1.30 (1)	C15-F7	1.27 (1)
C10-F2	1.29 (1)	C15-F8	1.32 (1)
C10-F3	1.31 (1)	C15-F9	1.29 (1)
C14-F4	1.28 (4)	C19-F10	1.26 (3)
C14-F5	1.26 (3)	C19-F11	1.29 (2)
C14-F6	1.30 (3)	C19-F12	1.29 (2)
C14-F4′	1.25 (6)	C19-F10′	1.24 (7)
C14-F5′	1.17 (9)	C19-F11′	1.27 (11)
C14-F6′	1.26 (3)	C19-F12′	1.25 (5)

(f) Bond Angles Involving Fluorine Atoms

F1-C10-F2	106 (1)	C11-C10-F1	112 (1)
F1-C10-F3	104 (1)	C11-C10-F2	113 (1)
F2-C10-F3	107 (1)	C11-C10-F3	114 (1)
F4-C14-F5	113 (3)	C13-C14-F4	114 (2)
F4-C14-F6	103 (2)	C13-C14-F5	112 (1)
F5-C14-F6	106 (3)	C13-C14-F6	108 (2)
F4′-C14-F5′	110 (6)	C13-C14-F4′	109 (4)
F4′-C14-F6′	102 (8)	C13-C14-F5′	114 (5)
F5′-C14-F6′	109 (7)	C13-C14-F6′	112 (3)
F7-C15-F8	106 (1)	C16-C15-F7	112 (1)
F7-C15-F9	106 (1)	C16-C15-F8	109 (1)
F8-C15-F9	108 (1)	C16-C15-F9	114 (1)
F10-C19-F11	107 (2)	C18-C19-F10	113 (2)
F10-C19-F12	104 (2)	C18-C19-F11	109 (1)
F11-C19-F12	112 (3)	C18-C19-F12	112 (2)
F10′-C19-F11′	101 (7)	C18-C19-F10′	112 (4)
F10′-C19-F12′	111 (6)	C18-C19-F11′	111 (2)
F11′-C19-F12′	110 (6)	C18-C19-F12′	111 (2)

[a] Standard deviations are in parentheses.

Table V. Deviations from Least-Squares Planes[a] for [Cu(hfac)$_2$(TMPO-OH)]

(a) Deviations from the Planes

plane 1 (n = 4): O2(0.03), O3(−0.03), O4(−0.02), O5(0.03), Cu(0.05)
plane 2 (n = 4): C1(0.00), C2(0.00), C4(−0.01), C5(0.07), N(−0.07), O1(−0.16), C3(0.22), O6(0.15)
plane 3 (n = 3): O1(0.00), C1(0.00), C5(0.00), N(0.04)
plane 4 (n = 7): O2(−0.01), O3(0.01), C10(0.01), C11(0.01), C12(0.00), C13(0.00), C14(−0.02), Cu(−0.13), F1(−1.15), F2(0.84), F3(0.25), F4(−0.07), F5(−0.89), F6(1.12), F4′(−1.10), F5′(0.14), F6′(0.83)
plane 5 (n = 7): O4(0.01), O5(−0.02), C15(−0.02), C16(0.00), C17(−0.02), C18(−0.01), C19(0.06), Cu(−0.12), F7(−1.09), F8(0.97), F9(0.09), F10(−0.54), F11(1.30), F12(−0.52), F10′(0.80), F11′(0.65), F12′(−1.09)

(b) Equations of the Planes[b]

plane	A	B	C	D
1	3.687	−6.798	12.910	−1.864
2	9.018	3.360	−9.578	−0.129
3	−9.513	3.046	8.191	−0.131
4	4.968	6.725	11.630	−1.600
5	2.448	6.818	13.840	−1.747

(c) Dihedral Angles (Deg) between Planes

planes	angle	planes	angle
1-2	89.2	2-4	81.6
1-3	85.8	2-5	96.0
1-4	7.8	3-4	93.5
1-5	7.2	3-5	78.7
2-3	155.5	4-5	15.0

[a] In section a, numbers in parentheses refer to the distance (Å) of the given atom from the calculated plane. The first n atoms in each case determine the given plane. [b] In the form $Ax + By + Cz = D$.

from the least-squares plane through the associated chelate ring (see Figures 1 and 2).

The observed geometry of the nitroxyl radical ligand is influenced to a large degree by the highly anisotropic thermal motion characteristic of all of the atoms of the TMPO–OH ligand. The severity of this motion is clear from an inspection of Figure 2 where it may also be noted that the preferred direction of motion for all atoms of the TMPO–OH group is approximately perpendicular to the mean plane of the radical ligand ring. Atoms O1, C2, and C4 and the four methyl groups on C1 and C5 seem particularly subject to motion of this type. As a result of this anisotropic motion of the atoms of the TMPO–OH ring, the conformation seen here for this tetramethylpiperidinyl-*N*-oxy derivative is quite different from the usual chair conformation flattened at the nitroxyl end seen in structures of similar radical species.[19] In the present structure, for example, the four atoms O1, N, C1, and C5 are almost planar, with the N–O1 bond making an angle of only 5 (1)° relative to the N–C1–C5 plane and N being displaced only 0.04 Å out of the O1–C1–C5 plane. Noncoordinated piperidinyl-*N*-oxy radicals are not normally flattened to this degree, with an angle of 16–22° between the N–O bond and the C–N–C plane being typical for these species. The Cu(II)–O1–N angle of 170.1 (5)° in the present structure is also much larger than would have been expected for coordination through a lone pair of electrons on an sp^2-hybridized nitroxyl oxygen atom.

The six-membered TMPO–OH nitroxyl radical ring does adopt the expected chair conformation but is much more flattened than normally seen, with atoms C3 and N being only +0.2 Å and −0.1 Å, respectively, out of the plane of the other four ring atoms. The large-scale thermal motion observed for the atoms of the TMPO–OH group, the unusual apparent flattening of this species, and the abnormal bond lengths seen within this ring (e.g., C3–C4 and C2–C3) suggest that the atoms of this radical ligand are disordered on a static or dynamic basis between two different TMPO–OH ring conformations. Corresponding unsubstituted (or partially substi-

---

[19] (a) Shibaeva, R. N. *J. Struct. Chem. (Engl. Transl.)* **1975**, *16*, 318. (b) McPhail, A. T.; Abou-Donia, M. B.; Rosen, G. M. *Mol. Pharmacol.* **1976**, *12*, 590.

tuted) piperidinyl-*N*-oxy radicals have been shown to rapidly interconvert between two conformations in solution.[20] While all atoms of the nitroxyl radical are clearly involved in this disorder phenomenon, the particularly large components of motion approximately perpendicular to the mean ring plane for C4, C2, O1, and the four methyl groups would seem to indicate that these atoms engage in the largest amount of motion during the conformational change taking place here. The flattening of the TMPO–OH ring observed in the present case is thus likely to be a direct consequence of the experimental observation of the "average" conformation based on the two unresolved disordered conformations likely to be present.

The measured magnetic moment for the title complex is 2.7 μ_B/mol of formula unit at room temperature (21 °C). This result suggests a surprisingly small magnetic interaction for a nitroxyl radical complex of a paramagnetic transition-metal ion. In contrast, other closely related systems such as Cu(hfac)$_2$·TMPO,[6] Cu(hfac)$_2$·DTBN (DTBN = di-*tert*-butyl nitroxide),[4b] and VO(hfac)$_2$·TMPO[7] exhibit strong antiferromagnetic interactions, with $|2J|$ on the order of 700 cm^{-1} in all three cases. Thus, the magnetic moment reported above for Cu(hfac)$_2$(TMPO–OH) suggests that this complex will be the first such species to show very little magnetic interaction between the unpaired electrons of the ligand and the paramagnetic metal atom. While the exact extent of the interaction between the two unpaired electrons in the present system remains to be determined by low-temperature magnetic susceptibility studies (currently in progress), the room-temperature magnetic moment clearly precludes the type of strong interaction seen in the cases cited above.

The near linearity of the Cu–O–N(nitroxyl) arrangement (Cu–O1–N = 170.1 (5)°) and the weakness of the copper(II)–nitroxyl bond (Cu–O1 = 2.439 (6) Å) are, presumably, primarily responsible for the lack of significant magnetic interaction between the unpaired electrons in this system. These two unpaired electrons presumably reside in orbitals of π^* symmetry (on nitroxyl) and $d_{x^2-y^2}$ symmetry (on Cu(II)). If the nitroxyl functional group were perfectly normal to the equatorial plane of the six-coordinate copper(II) ion, the resultant zero overlap between the orbitals would cause any magnetic interaction between the unpaired electrons to be small and ferromagnetic in nature. For a nitroxyl complex involving a strongly bent metal–nitroxyl bonding arrangement, nonzero overlap between these orbitals would be expected to lead to a pronounced antiferromagnetic interaction between the unpaired electrons. On this basis, the nearly linear Cu–O1–N angle seen in the present structure is consistent with a very small magnetic interaction and the observed room-temperature magnetic moment reported above.

The six-coordinate nature of this adduct in the solid state also may contribute to the weakness of the metal–nitroxyl bond and the weakness of the magnetic interaction. In a square-pyramidal five-coordinate adduct such as Cu(hfac)$_2$·TMPO, the copper(II) ion would normally be found displaced 0.1–0.2 Å above the basal plane of coordinating atoms in the direction of the nitroxyl radical apical ligand, as has been found in other square-pyramidal systems.[17,21,22] This apical displacement would allow formation of a significantly stronger bond between copper(II) and the nitroxyl radical than is seen in the present six-coordinate case, where the copper atom is actually found 0.05 Å out of the O2–O5 plane in the direction of the coordinating hydroxyl group.

Thus, the near linearity of the Cu–O1–N(nitroxyl) interaction and the six-coordinate nature of the metal-atom environment (with the resultant weak Cu–O1 bond) seen in the present case are important in establishing the degree of magnetic interaction present in the Cu(hfac)$_2$·TMPO–OH complex. The structural variations associated with the large differences in the magnitude of the magnetic interaction for this adduct and for those adducts which exhibit large antiferromagnetic interactions (see above) will be the subject of further study in this laboratory.

Acknowledgment. The authors wish to thank Professor R. S. Drago for providing the results of the elemental analysis of the title compound. Computing funds for this work were provided by Colorado State University and the Colorado State University Computing Center.

Registry No. Cu(hfac)$_2$(TMPO–OH), 72692-66-1; Cu(hfac)$_2$, 14781-45-4.

Supplementary Material Available: Table VI, a listing of observed and calculated structure factor amplitudes (×10) for Cu(hfac)$_2$)-(TMPO–OH) (10 pages). Ordering information is given on any current masthead page.

---

(20) (a) Janzen, E. G. *Top. Stereochem.* **1971**, *6*, 177. (b) Rolfe, R. E.; Sales, K. D.; Utley, J. H. P. *J. Chem. Soc., Perkin Trans. 2* **1973**, 1171.

(21) Bushnell, G. W. *Can. J. Chem.* **1971**, *49*, 555.

(22) Jose, P.; Doni, S.; Fernando, O. *J. Inorg. Nucl. Chem.* **1969**, *31*, 1971.